

Dynamic User Association based on Fractional Frequency Reuse

Ilhak Ban and Se-Jin Kim[†]

Abstract

This paper proposes a novel fractional frequency reuse(FFR) based on dynamic user distribution. In the FFR, a macro cell is divided into two regions, i.e., the inner region(IR) and outer region(OR). The criterion for dividing the IR and OR is the distance ratio of the radius. However, these distance-based criteria are uncertain in measuring user performance. This is because there are various attenuation phenomena such as shadowing and wall penetration as well as path loss. Therefore, we propose a novel FFR based on dynamic user classification with signal to interference plus noise ratio(SINR) of macro users and classify the FFR into two regions newly. Simulation results show that the proposed scheme has better performance than the conventional FFR in terms of SINR and throughput of macro cell users.

Keywords : OFDMA, FFR, User Association, SINR, Capacity

1. Introduction

In the fifth generation networks, To increase the capacity of the cell, more small cells will be added. However, Inter-cell interference will increase and the amount of available resources is insufficient^[1,2]. For these reasons, performance deterioration of the cellular network occurs. Therefore, how to mitigate interference and management resource is an important problem in the cellular network^[3,4].

In the cellular networks, signal-to-interference noise plus ratio(SINR) is used as an indicator of cellular network performance. Therefore, it is applied to the interference model using the distance between macro user equipment(MUE) and macro base station(MBS). Accordingly, the received signal strength is weakened when the user is far from the MBS, and the user is susceptible to interference from neighboring the MBS with using same subchannel, resulting in performance degradation. This interference is referred to as co-channel interference(CCI)^[5,6]. The fractional frequency reuse (FFR) method has been proposed to address this interference. In the FFR, frequency bands are used differently in each region to eliminate intra-cell interference.

The FFR is used to reduce the interference of the same channel, thereby increasing the SINR and capacity. The FFR have reuse-1 and reuse-3 to increase user throughput^[7,8]. In the traditional FFR method, users are divided into the IR and the OR according to distance. The closer the MUE is to the MBS, the reuse-1 is used, and the further away from base station the reuse-3 is used^[9,10]. There were various analyzes of the IR and the OR classification in^[11-14]. In^[11,12], they have classification using the distance between the MBS and MUE for dividing the cell region into two regions based on the FFR. However, in a real environment, it is not appropriate to determine the location of the UE in terms of distance by interference and shadowing due to various buildings and walls. In addition, additional geographic information is required. In^[13], users in the cell as divided the IR and the OR according to the average SINR and the classification threshold of small area. In^[14], they divided the UEs in the IR and the OR by reference signal strength. If the received signal strength from serving MBS is 3dB higher than that of neighboring MBSs, the user is classified as the IR. Otherwise, it is classified the OR.

Since the SINR varies with the location of the UEs, this affects system performance. In this paper, we propose a novel FFR scheme based on MUE's SINR. Using this method, the location of MUEs in the IR and the OR of the FFR is more realistically distinguished.

The composition of this paper is as follows. Chapter 2 shows the system model. Chapter 3 explains the pro-

Department of Computer Science & Statics, Chosun University, Gwangju, Korea

[†]Corresponding author : sjkim@chosun.ac.kr
(Received : March 11, 2020, Revised : March 14, 2020,
Accepted : March 17, 2020)

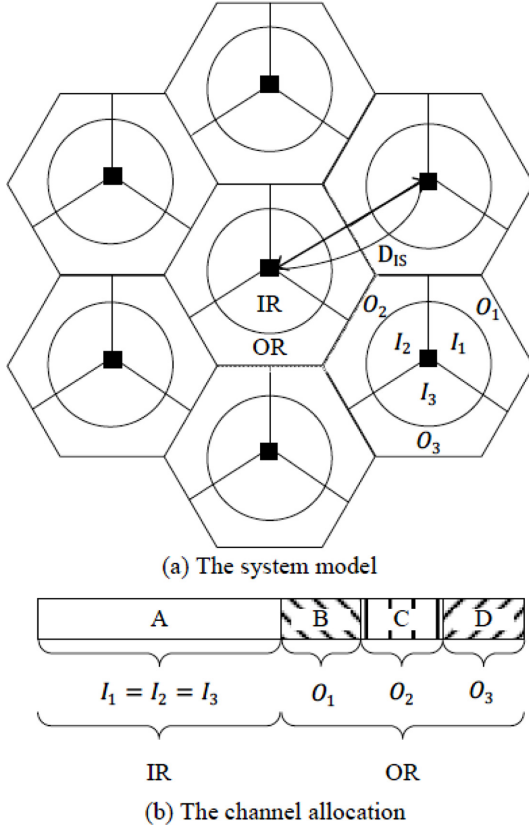


Fig. 1. The system model and the channel allocation with FFR.

posed scheme of classifying the MUEs. Section 4 shows the performance comparison with existing frequency reuse methods and concludes with Chapter 5.

2. System Model

We consider the downlink of a cellular network with orthogonal frequency division multiple access (OFDMA)-frequency division duplex (FDD). Fig. 1 shows that the system model and the channel allocation for FFR. Fig. 1-(a) shows the system topology and channel allocation with the FFR scheme. We assume that a set of M MBSs, $\mathbf{M} = \{1, \dots, M\}$ and each MBS is located at the center of each cell. Every cell consists of 19 cells, from the target cell to the surrounding two-tier cell. Each cell has three directional antennas so divided as three sectors. In the FFR, each sector has two regions, the IR and the OR, respectively. These two areas are marked as I and O , respectively. Furthermore, a set of

N MUEs, $\mathbf{N} = \{1, \dots, N\}$ is uniformly deployed per sector in each cell. The MBS assigns a set of K subchannels, $\mathbf{K} = \{1, \dots, K\}$ to the UEs. Fig. 1-(b) shows the channel allocation in the FFR. Users in the IR (I_1, I_2, I_3) are allocated channel A, which is $\lfloor \frac{3K}{6} \rfloor$ of the total channel. $\lfloor \cdot \rfloor$ is a floor function. On the other hand, users in the OR (O_1, O_2, O_3) are allocated channels B, C, and D, which are $\lfloor \frac{K}{6} \rfloor$ for each sector, respectively.

We use COST231-Hata model to calculate the path loss (PL) between the MBS and MUE. COST231-Hata model is an extension of the Hata model, which increases frequency operation up to 2 GHz. The main parameters of the COST231-Hata model are expressed as follows^[15].

$$PL[dB] = A - a(h_m) + B \log_{10}(d) + C \quad (1)$$

where $A = 46.3 + 33.9 \log_{10}(f) - 13.82 \log_{10}(h_b)$, $a(h_m) = (1.1 \log_{10}(f) - 0.7)h_m - 1.56 \log_{10}(f)0.8$, and $B = 44.9 - 6.55 \log_{10}(h_b)$. f is the carrier frequency in MHz. h_m and h_b are mobile and base station antenna height in m, respectively. d is distance between serving base station and user in m. $a(h_m)$ is used in small and medium size city as mobile antenna correction factor. C is area correction factor, 0 dB in the medium sized city and suburban, and 3 dB in the metropolitan city.

We calculate the SINR of MUE n in the IR served by MBS m on subchannel k , expressed as

$$Y_{mnk} = \frac{P_{mnk} PL_{mnk} \omega_{mnk} A(\theta)}{\sigma^2 + \sum_{j \in \mathbf{M}, j \neq m} P_{jnk} PL_{jnk} A(\theta)} \quad (2)$$

where P_{mnk} is the transmission power between the MBS m and MUE n on subchannel k . Further, P_{jnk} is the transmission power and channel gain between neighboring MBS j and MUE n on subchannel k . ω_{mnk} is an indicator variable, if MBS m allocate subchannel k to MUE n , $\omega_{mnk} = 1$ and 0 otherwise. In addition, σ^2 is the white noise power and $A(\theta)$ is azimuth antenna pattern between the MBSs m and MUEs n , can be expressed as

$$A(\theta) = A_g - \min \left[12 \left(\frac{\theta}{\theta_{3dB}} \right)^2, A_m \right], -\pi \leq \theta \leq \pi \quad (3)$$

where A_g and A_m are the maximum antenna gain and the maximum attenuation, respectively. θ_{3dB} is 3dB beam-width^[16].

We calculate the spectral efficiency for MUE n served by MBS m on subchannel k , γ_{mnk} , is obtained by

$$\gamma_{mnk} = \begin{cases} 0 & \text{if } S_E(\gamma_{mnk}) < r_{min} \\ S_E(\gamma_{mnk}) & \text{if } r_{min} \leq S_E(\gamma_{mnk}) \leq r_{max} \\ r_{max} & \text{if } r_{max} < S_E(\gamma_{mnk}) \end{cases} \quad (4)$$

where $S_E(\gamma_{mnk}) = \log_2(1 + \eta\gamma_{mnk})$ in bps/Hz and $\eta = 1.5 / \ln(5P_e)$ with the target bit error rate P_e ^[17]. Furthermore, when r_{min} and r_{max} are the minimum and maximum SINR in dB, respectively^[18], $r_{min} = S_E(r_{min})$ and $r_{max} = S_E(r_{max})$ are the minimum and maximum spectral efficiencies in bps/Hz, respectively^[19].

Through the SINR γ_{mnk} in (2), the capacity of MUE n served by MBS m on subchannel, can be expressed as

$$C_{mnk} = BW \sum_{\forall k \in K} \log_2(1 + \gamma_{mnk}) \quad (5)$$

where BW is the bandwidth of a subchannel in Hz.

3. Proposed Scheme

In this section, we propose a new FFR scheme based on user SINR to determine the IR and the OR over a dB threshold γ_{th} . Fig. 2 shows the flow chart of this proposed scheme. Let Γ_{mn} denote the SINR of MUE n served by MBS m in the IR. Γ_{mn} can be obtained by

$$\Gamma_{mn} = \frac{P_{mn} P_{Lmn} A(\theta)}{\sigma^2 + \sum_{j \in M, j \neq m} P_{jn} P_{Ljn} A(\theta)} \quad (6)$$

Let α_{mn} denote an indicator variable, $\alpha_{mn} = 1$ if MUE n served by MBS m is a member of the IR, and 0 is a member of the OR. If SINR of MUE is greater than or equal to the given threshold, the MUE is considered as the IR. Conversely, if the SINR is smaller than the threshold, it is regarded as the OR, α_{mn} can be obtained by

$$\alpha_{mn} = \begin{cases} 1 & \text{if } \Gamma_{mn} \geq \gamma_{th} \\ 0 & \text{otherwise} \end{cases} \quad (7)$$

where γ_{th} is a given target SINR threshold for dividing MUEs between the IR and OR.

In the FFR, system throughput is different because it uses different resources depending on the number of the IR and the OR users. Accordingly, the IR and the OR capacity are calculated using the SINR of each UE,

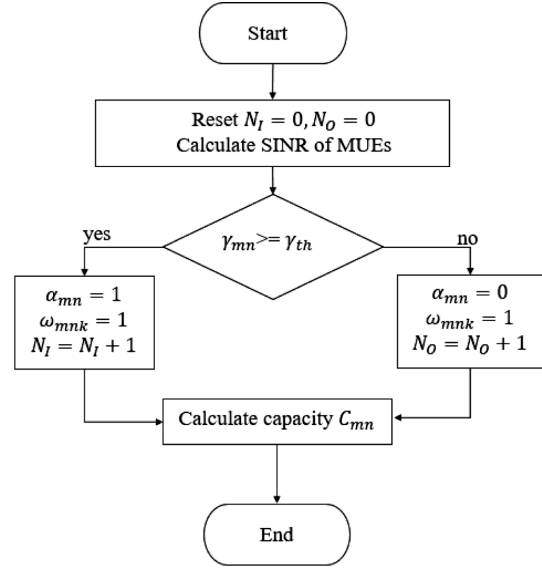


Fig. 2. The flow chart of the proposed FFR scheme.

respectively. The number of subchannels in each region depends on the number of newly defined users. Let $N_I = \sum_{n \in N} \alpha_{mn}$ and $N_O = N - N_I$ denote the numbers of MUEs in the IR and OR in each cell site, respectively. After dividing the MUE in the IR and OR, the MBS assigns subchannels to MUEs in the IR and OR. For this MUE in the IR and OR, MBS m assigns $\lfloor \frac{3K}{6N_I} \rfloor$ and $\lfloor \frac{K}{6N_O} \rfloor$ subchannels to each MUE in the IR and OR by setting $\omega_{mnk} = 1$, respectively.

4. Simulation Results

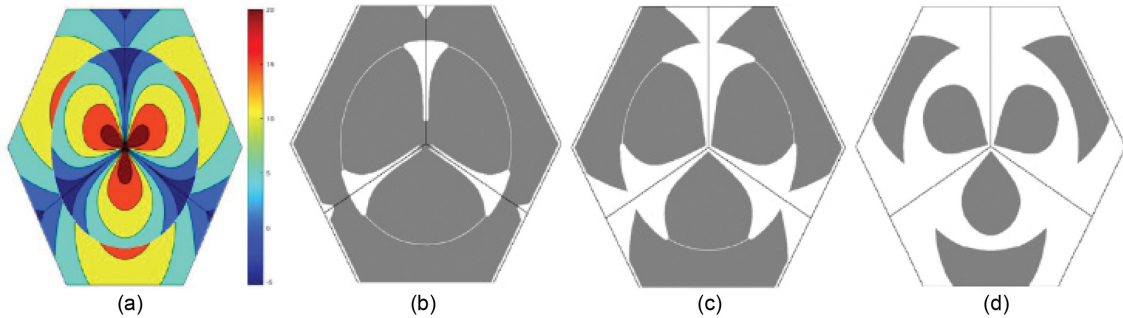
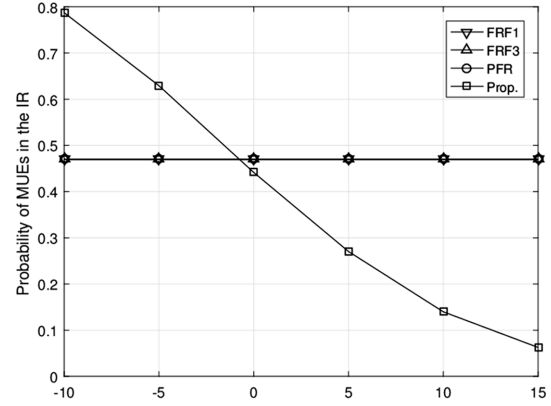
In this section, we evaluate the system performance of the proposed scheme with frequency reuse factor 1 (FRF1), frequency reuse factor 3 (FRF3) and FFR^[20] using distance threshold in terms of MUE count probability, mean MUE SINR and mean MUE capacity using a Monte Carlo simulation. The cell layout is shown in Fig. 1. We compare the proposed scheme with FRF1, FRF3 and the FFR. The transmission power of MBSs with FRF1 and FRF3 is 20W while with the FFR is 15W in the IR and 22W in the OR, respectively. We deploy the MUE $N = 30$ in a sector. In the FRF1 and FRF3, the number of subchannels used in one sector is equal to $\lfloor \frac{K}{N} \rfloor$ and $\lfloor \frac{K}{N/3} \rfloor$, respectively. On the other

Table 1. System parameter

Parameter	Value
Carrier frequency	2.0GHz
Total bandwidth	10MHz
Number of subchannels (K)	1000
Bandwidth per subchannel	10kHz
Inter site distance (D_{IS})	500m[16]
BS Transmission power	w/o FFR: 20W, FFR IR: 15W, FFR OR: 22W[20]
Number of UEs per sector (N)	30
Mini distance between the MBS and MUEs	35m[16]
σ^2	-174dBm/Hz
A_g	14dB[16]
A_m	20dB[16]
θ_{3dB}	70°[16]
Min and Max SINR ($\gamma_{\min}, \gamma_{\max}$)	-10, 18.5dB[18]
Min and Max spectral efficiency (r_{\min}, r_{\max})	0.137, 4.4bps/Hz[19]
P_e	10^{-3} [17]
Given SINR threshold (γ_{th})	-10 ~ 15dB

hand, in the FFR and proposed scheme, the number of subchannels used in the IR and the OR in a sector is $\lfloor \frac{3K}{6N_I} \rfloor$ and $\lfloor \frac{K}{6N_O} \rfloor$. We consider the SINR threshold γ_{th} from -10dB to 15dB to maximize the system capacity. We use a log-normal shadow fading with zero mean and standard deviation of 8dB. Other parameter is shown in Table 1.

Fig. 3 shows that the heat map of the FFR scheme and the user distribution of the proposed scheme with γ_{th} . Fig. 3-(a) shows the heat map of the FFR. Each IR

**Fig. 3.** The heat map of the FFR scheme and the user distribution of the proposed scheme with γ_{th} .**Fig. 4.** The probability of MUEs in the IR.

and OR user classification distribution based on distance. The inner part of the circle is the IR part. There are some users who have poor performance in the IR (blue color). This is because interference effects on the user location. Thus, we distinguish between the IR and OR using the MUE's SINR with various dB thresholds. Fig. 3-(b), (c) and (d) show the IR and OR user distribution of the proposed scheme according to the threshold $\gamma_{th} = 0, 5,$ and 10 dB, respectively. Here, the black part is classified as the IR user and the white part is classified as the OR user. If the threshold γ_{th} is set high, most of the users belong to the IR. Therefore, according to the dB threshold γ_{th} , distribution of users in the IR and OR is different. The users in the IR decrease as γ_{th} increase.

Fig. 4 shows the probability of MUEs in the IR. The probability of UEs in the OR is drawn in the opposite way. In the FFR3, there is no criterion for dividing the IR and the OR, but in this simulation, we use 0.63 to represent the same proportion of users. In the FFR3 and

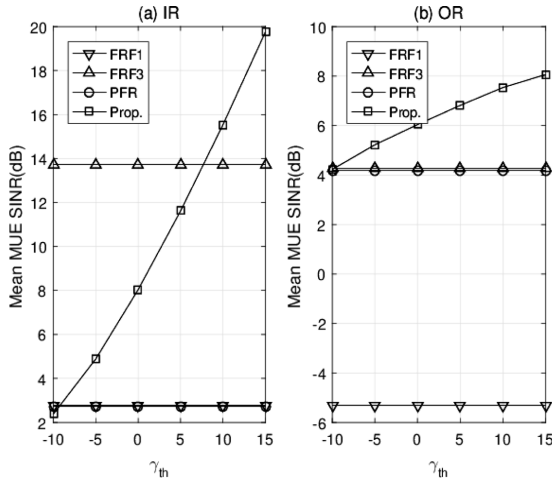


Fig. 5. Mean MUE SINR in the IR and OR.

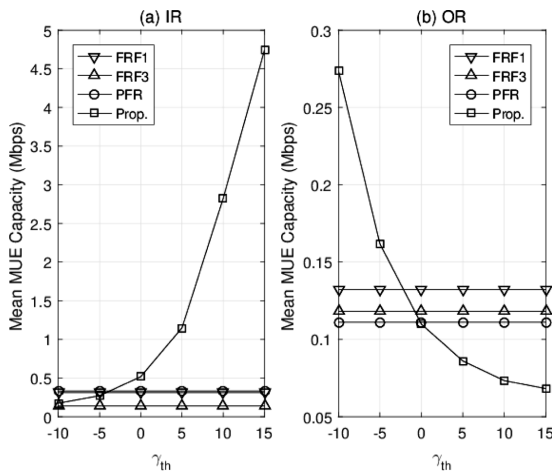


Fig. 6. Mean MUE capacity in the IR and OR.

the FFR, the IR and OR are divided by 0.63 times of the cell radius, so the ratio of users in the IR is fixed at 47%. In the proposed scheme, the number of MUEs in the IR is gradually decreased when $\gamma_{th} \geq -1$ dB.

Fig. 5 shows the mean SINR of MUEs in the IR and OR as γ_{th} increases. FRF3 has the highest SINR because the amount of CCI is smaller than that of the FFR. On the other hand, in the FFR method, since the CCI in the IR using Reuse-1 is higher than the FRF3, the average SINR is low. The proposed method is similar to FRF3 because the amount of CCI decreases as γ_{th} increases and the number of UE in the IR decreases. In the IR, the proposed scheme has better performance than the FFR and FRF1 schemes when $\gamma_{th} \geq -8$ dB while the

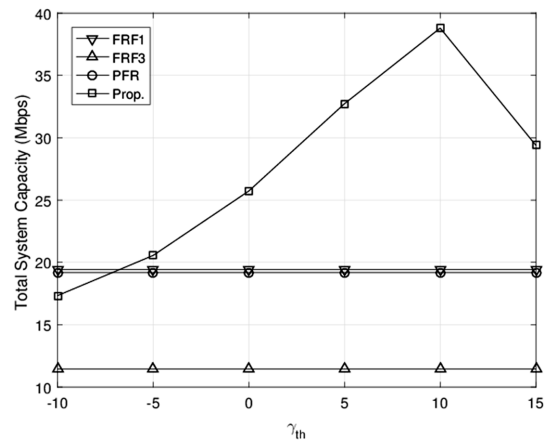


Fig. 7. Total system capacity.

FRF3 scheme when $\gamma_{th} \geq 8$ dB. On the other hand, in the OR, the proposed scheme has always higher performance than other schemes while the FRF1 scheme has the worst performance because of strong CCI.

Fig. 6 shows the results of mean MUE capacity in the IR and OR according to the γ_{th} threshold. In the IR, FRF3 has the worst performance since the MBS assigns $\lfloor \frac{K}{N/3} \rfloor$ subchannels to each MUE while it assigns $\lfloor \frac{K}{N} \rfloor$ and $\lfloor \frac{3K}{6N_f} \rfloor$ subchannels to each MUE in the FRF1 and FFR schemes, respectively. The proposed scheme increases as γ_{th} increases and those are higher than other schemes from $\gamma_{th} \geq -4$ dB. On the other hand, in the OR, the FFR scheme has the worst performance since the MBS assigns $\lfloor \frac{K}{6N_o} \rfloor$ subchannels to each MUE while it assigns $\lfloor \frac{K}{N} \rfloor$ and $\lfloor \frac{K}{N/3} \rfloor$ subchannels to each MUE in the FRF1 and FRF3 schemes, respectively. The proposed scheme decrease as γ_{th} increases and those are lower than other schemes when $\gamma_{th} \geq 0$ dB.

Fig. 7 shows the results of the total system capacity as γ_{th} increases. The FRF3 scheme has the worst performance since the MBS assigns subchannels $\lfloor \frac{K}{N/3} \rfloor$ to each MUE. On the other hand, the results of the proposed scheme increase as γ_{th} increases and the proposed scheme outperforms other schemes when $\gamma_{th} \geq -7$ dB. In addition, the results of the proposed scheme are approximately twice higher than those of the FRF1 and FFR

schemes when $\gamma_{th}=10\text{dB}$. Meanwhile, the results of the proposed scheme are 32% higher than those of the FRF1 and FFR schemes when $\gamma_{th}=0\text{dB}$ but the performance of the mean MUE capacity for the proposed scheme is higher than other schemes in the IR while those are the same as the results of the FFR scheme in the OR, as shown in Fig. 6.

5. Conclusion

In this paper, we proposed a novel dynamic user FFR scheme based on the SINR to increase the system performance. The conventional FFR determines UE to the IR and OR based on UE distance. However, this scheme is not suitable for the real world. Simulation results show that the performance improvement over the distance based FFR in terms of average SINR and capacity after the threshold of -5dB . However, this paper does not consider the fairness between the IR and OR users. In addition, dynamic resource allocation can also be considered due to differences in the number of users in IR and OR. Therefore, for future work, we are planning to study a dynamic channel assignment scheme to improve the system performance and consider fairness.

Acknowledgments

This work was supported by the National Research Foundation of Korea (NRF) grant funded by the Korea government (MSIT) (No. 2019R1H1A1101960).

References

- [1] M. Kamel, W. Hamouda, and A. Youssef, "Ultra-dense networks: A survey," *IEEE Commun Surveys Tuts*, vol. 18, no. 4, pp. 2522–2545, 4th Quart., 2016.
- [2] A. Damnjanovic, J. Montojo, Y.-B. Wei, T.-F. Ji, T. Luo, M. Vajapeyam, T.-S. Y, O. Song, D. Malladi, "A survey on 3GPP heterogeneous networks," *IEEE Wireless Commun.*, vol. 18, no. 3, pp. 10–21, Jun. 2011.
- [3] N. Himayat, S. Talwar, A. Rao, and R. Soni, "Interference management for 4G cellular standards," *IEEE Commun. Mag.*, vol. 48, no. 8, pp. 86–92, Aug. 2010.
- [4] P.-G. Lee, T.-Y. Lee, J.-K. Jeong, and J.-T. Shin, "Interference management in LTE femtocell systems using Fractional Frequency Reuse," *ICACT, Phoenix*, vol.2, pp.1047-1051, Feb 2010.
- [5] 3GPP TSG-RAN WG1 Meeting #44, R1-060670, Siemens, "Interference mitigation by partial frequency reuse," February 2006.
- [6] G. Boudreau, J. Panicker, N. Guo, R. Chang, N. Wang, and S. Vrzic, "Interference coordination and cancellation for 4G networks," *IEEE Commun. Mag.*, vol. 47, no. 4, pp. 74–81, Apr. 2009.
- [7] A. Daeinabi, K. Sandrasegaran, and X.-P. Zhu, "Survey of icc mitigation techniques in lte downlink networks," in *ATNAC 2012*, Nov, pp. 1–6.
- [8] C. Kosta, B. Hunt, A.-U. Qaddus, and R. Tafazolli, "On interference avoidance through inter-cell interference coordination (ICIC) based on OFDMA mobile systems," *IEEE Commun. Surveys Tuts.*, vol. 15, no. 3, pp. 973–995, Mar. 2013.
- [9] T.-D. Novlan, R.-K. Ganti, A. Ghosh, and J.-G. Andrews, "Analytical Evaluation of Fractional Frequency Reuse for OFDMA Cellular Networks," *IEEE Trans. Wireless Commun.*, vol. 10, no. 12, pp. 4294–4305, December 2011.
- [10] T.-D. Novlan, R.-K. Ganti, A. Ghosh, and J.-G. Andrews, "Analytical Evaluation of Fractional Frequency Reuse for Heterogeneous Cellular Networks," *IEEE Trans. Commun.*, vol. 60, no. 7, pp. 2029–2039, July 2012.
- [11] M. Assad, "Optimal fractional frequency reuse (FFR) in multicellular OFDMA system," in *IEEE Vehicular Technology Conference*, September 2008, pp. 1–5.
- [12] T. Novlan, J.-G. Andrews, I.-S. Sohn, R.-K. Ganti, and A. Ghosh, "Comparison of fractional frequency reuse approaches in the OFDMA cellular downlink," in *Proc. IEEE Globecom*, Dec. 2010, pp. 1–5.
- [13] D. Gonzalez G, M.-G. Lozano, S.-R. Ruiz, and J. Olmos, "An analytical view of static intercell interference coordination techniques in OFDMA networks," in *2012 IEEE Wireless Communications and Networking Conf.*
- [14] D.-L. Perez, H. Claussen, and L. Ho, "Improved frequency reuse schemes with horizontal sector offset for LTE," in *Proc. IEEE PIMRC*, Sep. 2013, pp. 2159–2164.
- [15] 3GPP TR 25.996 V10.0.0, "Spatial channel model for Multiple Input Multiple Output (MIMO) simulations," Mar. 2011.
- [16] R4-092042, 'Simulation Assumptions and Parameters for FDD HeNB RF Requirements', 2009.
- [17] X.-X. Qiu and K. Chawla, "On the performance of

- adaptive modulation in cellular systems,” IEEE Transactions on Communications, vol. 47, no. 6, pp.884-895, 1999.
- [18] S.-J. Kim, “Dynamic Channel Assignment with Consideration of Interference and Fairness for Dense Small-cell Networks,” IEICE Transactions on Fundamentals of Electronics, Communications and Computer Sciences, Vol.E101-A, No.11, pp. 1984-1987, 2018.
- [19] S.-J. Kim and S.-H. Bae, “Interference-Aware Dynamic Channel Assignment Scheme for Enterprise Small-cell Networks,” IEICE Transactions on Communications, vol.E101B, no.12, pp.2453-2461, 2018.
- [20] T.-Y. Lee, H.-T. Kim, J.-H. Park, J.-T. Shin, “An Efficient Resource Allocation in OFDMA Femto-cells Networks,” IEEE Vehicular Technology Conference 2010 Fall, pp.1-5, 2010.